Spectroscopic and Computational Studies of Ground State Thermodynamic Equilibrium of s-Trans and s-Cis Conformers in *trans,trans*-1,4-Diphenyl-1,3-butadiene

Christopher E. Bunker, Cory A. Lytle, Harry W. Rollins, and Ya-Ping Sun*

Department of Chemistry, Howard L. Hunter Chemistry Laboratory, Clemson University, Clemson, South Carolina 29634-1905

Received: July 25, 1996[⊗]

At excitation wavelengths in the extreme red onset region of the *trans,trans*-1,4-diphenyl-1,3-butadiene (DPB) absorption spectrum, observed fluorescence spectra are mixtures of contributions from *s*-trans and *s*-cis conformers. Quantitative separations of the spectral mixtures by use of a chemometric method make it possible to determine relative fluorescence contributions and fluorescence quantum yields of DPB conformers as a function of temperature. Enthalpy differences of 1.9 and 2.3 kcal/mol are obtained for the ground state conformational equilibrium of DPB in methylcyclohexane and toluene, respectively. In computational studies, conformational energies and geometries of DPB are evaluated in terms of an *ab initio* method. The calculated s-cis−s-trans energy difference is in surprisingly good agreement with the experimental results.

Introduction

Linear polyenes and diphenylpolyenes have been studied extensively as models for photobiological systems and novel materials.[1] Significant progress has been made in the understanding of their somewhat unique electronic structures. It is generally accepted[1−4] that the photophysical and photochemical properties of these molecules are dictated by two low-lying excited singlet states ^{1}Bu* and ^{1}Ag*, which are one-photon and two-photon allowed, respectively, and that relative energies of the two excited states are dependent on the polyene chain length and on the solvent environment. For *trans,trans*-1,4-diphenyl-1,3-butadiene (DPB), available experimental results indicate that the one-photon-allowed ^{1}Bu* state is the lowest excited singlet state in a room-temperature solution, responsible for both absorption and emission.[3−6] The excited singlet state processes of DPB were studied in the gas phase under isolated molecular conditions, and the nonradiative decay was attributed to photoisomerization.[3,4,7,8] There has also been a number of time-resolved fluorescence and transient absorption studies of DPB excited singlet state lifetimes under different solvent conditions.[3,4,7,9−13] The solvent dependence of observed nonradiative decay rate constants are explained in terms of solvent effects of photoisomerization which involves large-amplitude molecular motion.

In addition to photoisomerization, the presence of ground state single-bond rotational conformers also plays a role in the photophysics and photochemistry of polyenes. In fact, ground state conformational equilibria in short-chain polyenes such as butadienes and hexatrienes have received much attention because of their structural relationships with vitamin-D derivatives.[14] For 1,3-butadiene, the s-trans and s-cis conformers and their thermodynamic equilibrium have been characterized by different methods,[15] including semiempirical and *ab initio* calculations at various levels.[16] The results suggest that the ground state energy of the s-cis conformer is ∼3 kcal/mol higher than that of the s-trans conformer in 1,3-butadiene, and the energy barrier separating the conformers is ∼7 kcal/mol (Scheme 1). Because absorption spectra of individual conformers are different, relative conformer excited state populations are dependent on excitation wavelength. The energy barrier separating the excited conformers apparently prevents conformational interconvertions during the excited state lifetimes of the conformers. As a result, effects of ground state conformational equilibria on product distributions in the photochemistry of 1,3-butadiene and related molecules follow Havinga's NEER (nonequilibrating excited rotamers) principle (Scheme 1).[18,19]

SCHEME 1

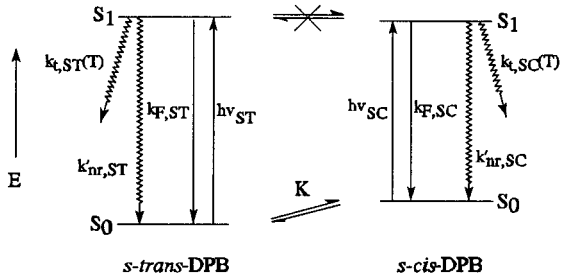

Recently, the presence of a ground state conformational equilibrium for DPB in a room-temperature solution and the adherence to the NEER principle were established experimentally,[20−22] following the report of a similar investigation of *all-trans*-1,6-diphenyl-1,3,5-hexatriene (DPH).[23] Because the equilibrium concentration of the minor conformer is low, the contribution of *s-cis*-DPB to the observed absorption spectrum is small, essentially buried under the intense spectrum of *s-trans*-DPB. Therefore, effects due to the presence of the s-cis conformer on observed fluorescence spectra become evident only when excitations are in the extreme red onset region of the observed DPB absorption spectrum.[20−22] Fluorescence spectra of the two conformers are also severely overlapping. The spectral mixtures can be separated into individual conformer spectra by applying chemometric methods to data matrices consisting of fluorescence spectra at a series of excitation wavelengths.[20,21] In this paper, we report a study in which fluorescence spectra and quantum yields of individual DPB conformers at different temperatures are obtained. The results make it possible to determine the thermodynamic parameters of the ground state conformational equilibrium. Experimental values of the enthalpy difference between DPB s-trans and s-cis conformers are compared to those from *ab initio* calculations.

[⊗] Abstract published in *Advance ACS Abstracts,* April 15, 1997.

S1089-5639(96)02271-2 CCC: $14.00

Experimental Section

Materials. *trans,trans*-1,4-Diphenyl-1,3-butadiene (Aldrich, 98%) was repeatedly recrystallized from ethanol. 9-Cyanoanthracene (Aldrich, 99%) was used as a fluorescence standard also after repeated recrystallization from ethanol. Hexane and toluene (Burdick and Jackson, spectrophotometry grade) and methylcyclohexane (Mallinckrodt, OR) were used as received.

Measurements. Absorption spectra were measured using a 1 cm cuvette on Shimadzu UV-2101PC and UV-3100 spectrophotometers. For the absorption spectra at different temperatures, measurements were carried out by placing the cuvette in a homemade sample holder that was thermostated through fluid circulation.

Fluorescence spectra were recorded on a Spex Fluorolog-2 photon-counting emission spectrometer equipped with a 450 W xenon source and an R928 photomultiplier tube in a cooled housing. A right-angle geometry was used. For measurements of fluorescence spectra at different temperatures, the sample holder that came with the instrument was replaced by a homemade sample holder that has the same geometry but allows fluid circulation for temperature variation and control. In order to reduce scattering associated with excitation in the extreme red onset region, fluorescence spectra were recorded using narrow excitation and emission slits (0.25 mm, 1 nm resolution). Fresh solutions were used in all measurements to minimize the effect of possible photochemical reactions. All fluorescence spectra were corrected for nonlinear instrumental response of the emission spectrometer using predetermined correction factors.

Fluorescence quantum yields of DPB in methylcyclohexane and toluene at different temperatures were determined on the basis of integrated spectral areas using 9-cyanoanthracene in hexane ($\Phi_F = 1.0$)[24] as a standard. Solutions used in fluorescence quantum yield measurements were deoxygenated by bubbling dry nitrogen gas for ~30 min. Effects due to changes in the index of refraction n from solvent to solvent were corrected as follows:

$$\Phi_{F,SP}/\Phi_{F,SD} = (F_{A,SP}/F_{A,SD})(n_{SP}/n_{SD})^{-2} \qquad (1)$$

where F_A represents the ratio between the integrated fluorescence spectral area and the optical density at the excitation wavelength, and SD and SP denote solvents for fluorescence standard and sample, respectively. Temperature variations in absorption and fluorescence measurements were accomplished through fluid circulation. A Haake K20 circulating bath and a DC3 controller were used to keep a sample solution at a constant temperature. The actual temperature of the sample solution was monitored by use of an Omega DP116-KCl digital thermometer and a temperature probe in contact with the solution in the cuvette through a small hole in the cap. The accuracy in temperature reading is ±0.1 °C.

Data Treatment and Calculation. Quantitative separations of fluorescence spectral mixtures of the conformers were accomplished by use of a chemometric method principal component analysis−self-modeling spectral resolution.[25−27] Applications of the method to DPB and DPH conformers have been described elsewhere.[21,23] Briefly, principal component analysis determines the number of significant components in a linear system.[28] For a data matrix **Y** consisting of n experimental fluorescence spectra of DPB at different excitation wavelengths, the analysis enables a representation of the spectra in a two-dimensional vector space because each observed spectrum is a linear combination of two pure conformer fluorescence spectra. The vector space can be constructed by two principal eigenvectors V_1 and V_2 of the matrix **Y**, which correspond to the two largest eigenvalues. For an observed spectrum Y_i in the data matrix,

$$Y_i = Y_i' + R_i = (\xi_{i1}V_1 + \xi_{i2}V_2) + R_i \qquad (2)$$

where Y_i' is the noise-attenuated spectrum regenerated from the two eigenvectors, and R_i is a residual vector containing primarily experimental noise. Because each spectrum in the data matrix is normalized in such a way that the area under the spectrum is unity, the combination coefficients ξ_{i1} and ξ_{i2} satisfy the following normalization condition,

$$\xi_1 \sum_{j=1}^{p} \nu_{1j}\Delta_j + \xi_2 \sum_{j=1}^{p} \nu_{2j}\Delta_j = 1 \qquad (3)$$

where ν represents elements of the eigenvectors, $\Delta = \lambda_{j+1} - \lambda_j$ (λ denotes wavelength), and p is the total number of wavelengths at which fluorescence intensities are used to form the data matrix.

The fluorescence spectrum of the s-trans conformer is known, and the spectrum of the s-cis conformer can be obtained from the eigenvectors in terms of a self-modeling spectral resolution method due to Lawton and Sylvestre.[29] With the determination of pure conformer spectra, fractional contributions of individual conformers to observed fluorescence spectra can be calculated.

$$(x_{SC}/x_{ST})_i = \frac{\begin{vmatrix} \xi_{ST1} & \xi_{i1} \\ \xi_{ST2} & \xi_{i2} \end{vmatrix}}{\begin{vmatrix} \xi_{i1} & \xi_{SC1} \\ \xi_{i2} & \xi_{SC2} \end{vmatrix}} \qquad (4)$$

where (ξ_{ST1},ξ_{ST2}) and (ξ_{SC1},ξ_{SC2}) are two sets of combination coefficients (subscripts 1 and 2 denote coefficients corresponding to principal components 1 and 2) for the s-trans (subscript ST) and s-cis (subscript SC) conformers, respectively, ξ_{i1} and ξ_{i2} are coefficients for the ith observed fluorescence spectrum in the data matrix, and x_{SC}/x_{ST} represents the ratio of fractional contributions of the two conformers. All calculations associated with the application of the principal component analysis−self-modeling spectral resolution method were performed on an IBM-compatible 486-50-MHz personal computer.

Computational studies of the energies and geometries of DPB conformers were carried out on a Silicon Graphics workstation. All semiempirical and *ab initio* calculations were performed in the environment of a commercial software package *Sparton* (version 3.0) from Wavefunction Inc.

Results

Conformer Fluorescence Spectra. Fluorescence spectra of *trans,trans*-1,4-diphenyl-1,3-butadiene (DPB) were measured as a function of excitation wavelength in methylcyclohexane (MCH) and toluene at room temperature (22 °C). When excitation wavelengths are within the main absorption band (280−350 nm) of DPB, observed fluorescence spectra due to emission from the s-trans conformer are excitation wavelength independent. The spectra corresponding to excitations at the absorption band maxima are shown in Figure 1. Observed absorption and emission spectra are only weakly solvent dependent, with the spectra in toluene slightly red-shifted from those in MCH. Somewhat more noticeable are changes in the absorption and fluorescence spectral profiles. Relative intensities of the vibronic peaks in the spectra are somewhat different in the two solvents.

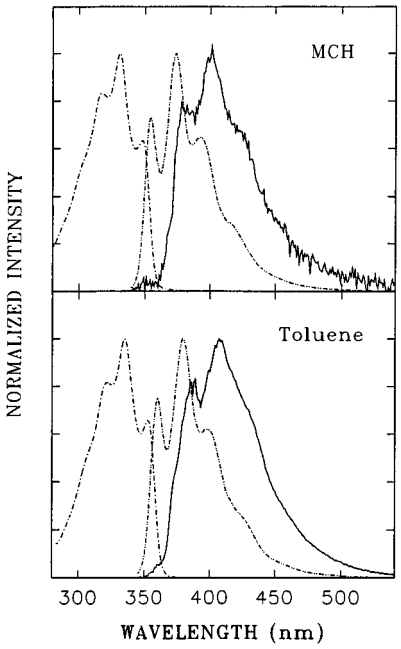

Figure 1. Absorption (-•-) and the s-trans (-•••-) and s-cis (—) conformer fluorescence spectra of DPB in MCH ($\lambda_{EXC} = 330$ nm) and toluene ($\lambda_{EXC} = 335$ nm) at room temperature ([DPB] = 2×10^{-6} M).

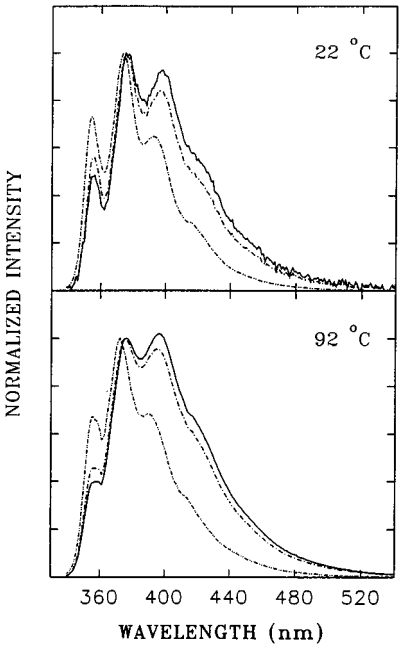

Figure 2. Observed fluorescence spectra of DPB in MCH at room (22 °C) and high (92 °C) temperatures with excitation wavelengths of 330 nm (-•••-), 367 nm (-•-), and 370 nm (—).

When excitation wavelengths are in the extreme red onset region, observed fluorescence spectra become very different from those of the s-trans conformer. In both solvents, the spectra are strongly excitation wavelength dependent. With a longer excitation wavelength, the observed fluorescence spectrum shows higher intensities at longer emission wavelengths, which are attributed to contributions of the s-cis conformer.[20,21] In order to obtain high-quality spectra for further chemometric treatments, special efforts were made in the experimental measurements. Because the excitation wavelengths in the extreme red onset region of the absorption spectrum are inside the emission spectral region, self-absorption becomes a problem when high DPB concentrations are used to maintain reasonable optical densities at the excitation wavelengths. On the other hand, the use of low DPB concentrations will result in significant excitation scattering effects on observed fluorescence spectra. A compromise for the two opposing factors was reached by use of a DPB concentration that corresponds to an optical density of ~0.7 at the first peak of the DPB absorption spectrum. Under such conditions, effects of excitation scattering are at a maangeable level, and the self-absorption can still be corrected. Factors for correcting self-absorption effects were generated by use of the fluorescence spectra excited at the absorption spectral maximum for concentrated and dilute DPB solutions, which correspond to optical densities of 0.7 and 0.05, respectively, at the first peak of the absorption spectrum. Corrected DPB fluorescence spectra in MCH thus obtained are shown in Figure 2, and the results in toluene are similar.

Fluorescence spectra of DPB were also measured as a function of excitation wavelength in MCH and toluene at a high temperature. The results are basically similar to those at room temperature. The same approach for balancing self-absorption and excitation scattering effects was used in the fluorescence measurements. As shown in Figure 2, the spectra at a high temperature are somewhat broader. With excitation wavelengths in the extreme red region, fluorescence spectra obtained at a high temperature have relatively higher intensities at longer emission wavelengths, corresponding to greater contributions from the s-cis conformer.

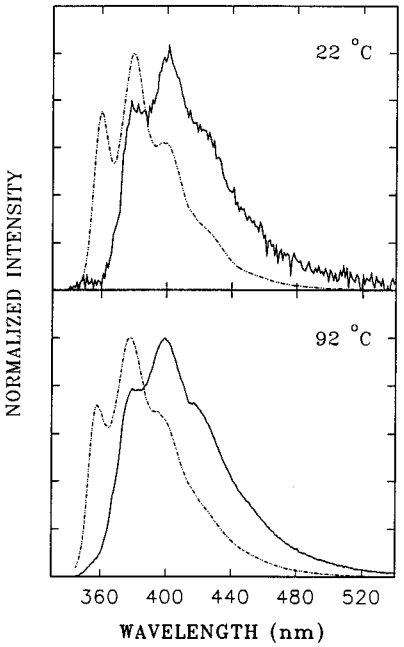

Figure 3. Fluorescence spectra of DPB s-trans (-•••-) and s-cis (—) conformers in MCH at room (22 °C) and high (92 °C) temperatures.

Observed fluorescence spectra corresponding to excitation wavelengths in the extreme red onset region of the DPB absorption spectrum are spectral mixtures of the s-trans and s-cis conformers. A determination of the pure fluorescence spectrum of s-cis-DPB was accomplished by use of a chemometric method principal component analysis−self-modeling spectral resolution.[21,23,25−29] The spectrum of the s-cis conformer in MCH is similar to that in hexane reported earlier.[21] As shown in Figure 3, the spectra of each conformer at two different temperatures are similar, except that the spectrum at the high temperature is slightly broader. The same results are obtained in toluene. A comparison of the s-cis spectra in MCH and toluene at room temperature is shown in Figure 1. Fractional contributions of the s-cis conformer to observed fluorescence spectral mixtures are shown in Table 1.

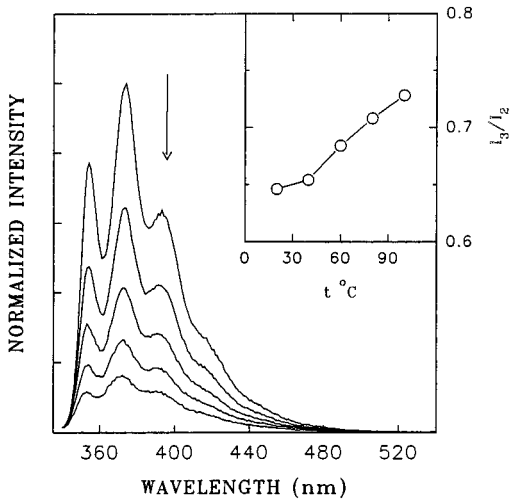

Figure 4. Observed fluorescence spectra of DPB in MCH (λ_{EXC} = 330 nm) at representative temperatures of (in the arrow direction) 20.8, 40.5, 60.2, 80.1, and 100.3 °C. The inset is a plot of the intensity ratio of the third and the second vibronic peaks as a function of temperature.

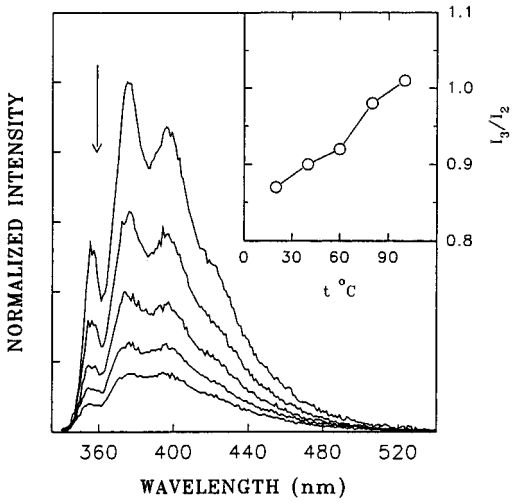

Figure 5. Observed fluorescence spectra of DPB in MCH (λ_{EXC} = 367 nm) at representative temperatures of (in the arrow direction) 20.8, 40.5, 60.2, 80.1, and 100.3 °C. The inset is a plot of the intensity ratio of the third and the second vibronic peaks as a function of temperature.

TABLE 1: Fluorescence Parameters of DPB s-Cis and s-Trans Conformers

solvent	λ_{EXC} (nm)	t (°C)	x_{SC} (%)	$\Phi_{F,OBS}$	$\Phi_{F,ST}$	$\Phi_{F,SC}$
hexane[21]	328	RT	0	0.37	0.37	
	365	RT	46	0.40		0.44
	368	RT	57	0.41		0.45
MCH	330	RT	0	0.393	0.393	
		92	0	0.098	0.098	
	367	RT	45	0.478		0.65
		92	56	0.114		0.13
	370	RT	57			
toluene	335	RT	0	0.192	0.192	
		93	0	0.0677	0.0677	
	371	RT	36	0.242		0.48
		93	45	0.083		0.11
	374	RT	46			

Temperature Dependence. Fluorescence spectra of DPB in MCH and toluene were measured as a function of temperature in the 20−100 °C range. Solutions used in the measurements were optically dilute (<0.1 at the excitation wavelength). At a given temperature, a solution was allowed to equilibrate for ∼15 min before fluorescence measurements were made. During that period, the sample was protected from the excitation source to minimize possible photodecomposition. At the excitation wavelength of 330 nm, observed fluorescence spectra of DPB in MCH are due exclusively to contributions of the s-trans conformer (Figure 4). The spectral profile is somewhat temperature dependent. As shown in the insert of Figure 4, relative vibronic peak intensities vary with temperature in a systematic fashion. The changes are due to an intrinsic temperature dependence of the s-trans conformer fluorescence spectrum.

For fluorescence spectra obtained at excitation wavelengths in the extreme red onset region of the DPB absorption spectrum, changes in spectral profile with temperature are due primarily to shifts in the thermodynamic equilibrium between the two conformers. However, intrinsic temperature dependencies of the conformer fluorescence spectra may also have some contributions. In order to study the temperature dependence of the conformational equilibrium, fluorescence spectra at different temperatures were obtained for DPB in MCH at 367 nm excitation and in toluene at 371 nm excitation. Shown in Figure 5 are representative spectra of DPB in MCH at different temperatures. A dependence of the observed spectral profile on temperature is evident.

A quantitative determination of the relative fluorescence contributions of the s-trans (x_{ST}) and s-cis (x_{SC}) conformers to observed spectral mixtures at different temperatures was accomplished by use of a linear least-squares regression method.

$$S_{OBS} = x_{ST}S_{ST} + x_{SC}S_{SC} \tag{5}$$

where S represents spectral vectors whose elements are fluorescence intensities at different wavelengths. The spectral vectors are normalized such that the area under each fluorescence spectrum is unity. Because the spectra of individual conformers are somewhat temperature dependent, the regression of an observed fluorescence spectrum at a given temperature requires pure conformer spectra at that same temperature. As an approximation, the s-cis conformer fluorescence spectra at different temperatures were obtained by linear interpolations from the spectra at room and high temperatures. In order to avoid empirical correction of the excitation scattering peak for every observed spectrum, regressions only cover the emission spectral wavelength range from 375 to 560 nm. Because in the treatment each spectrum is normalized with respect to the covered wavelength range, calculated relative contributions ($x_{SC,375}$ and $x_{ST,375}$) must be adjusted to those representing the whole fluorescence spectrum. From the normalized pure conformer fluorescence spectra, the ratio of integrated fluorescence spectral areas of the s-trans and s-cis conformers for the wavelength range 375−560 nm is r. Thus, the adjustment was made as follows:

$$x_{SC}/x_{ST} = \frac{1}{r}(x_{SC,375}/x_{ST,375}) \tag{6}$$

Fractional contributions of the s-tans and s-cis conformers to the observed fluorescence spectral mixtures in MCH and toluene are shown in Figure 6. Obviously, x_{SC} values increase with increasing temperature.

Quantum Yields. Fluorescence quantum yields of DPB in room-temperature (22 °C) MCH and toluene were determined at different excitation wavelengths. In experimental measurements of the yields at excitation wavelengths in the extreme red onset region of the DPB absorption spectrum, optical densities of 0.05−0.1 (in a 1 cm square cuvette) at the excitation wavelengths were used. The high DPB concentrations required to achieve these optical density values result in self-absorption

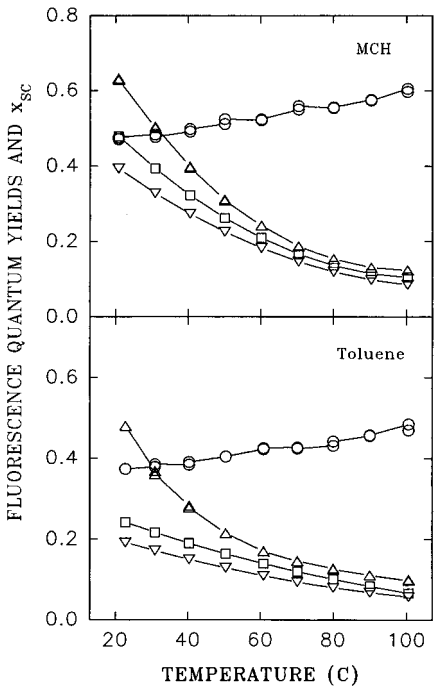

Figure 6. Fractional fluorescence contributions of *s-cis*-DPB (○), and fluorescence quantum yields of *s-trans*-DPB (▽), *s-cis*-DPB (△), and observed total emission (□) in MCH (λ_{EXC} of 330 nm for *s-trans*-DPB and 367 nm for others) and toluene (λ_{EXC} of 335 nm for *s-trans*-DPB and 371 nm for others) as a function of temperature.

effects that severely distort the blue onset portion of the observed fluorescence spectra. However, because the fluorescence spectral profile is concentration independent,[21] the blue portions of the spectra were corrected by use of the spectra obtained at the same excitation wavelengths but much lower DPB concentrations. The fluorescence quantum yields thus obtained are shown in Table 1. The yields at excitation wavelengths in the main absorption band are due exclusively to the s-trans conformer, $\Phi_{F,ST}$. If $\Phi_{F,ST}$ is assumed to be excitation wavelength independent, fluorescence quantum yields of the s-cis conformer $\Phi_{F,SC}$ can be determined from the equation as follows:[21]

$$\Phi_{F,SC}/\Phi_{F,ST} = (x_{SC}/x_{ST})\left[\frac{1+(x_{SC}/x_{ST})}{(\Phi_{F,OBS}/\Phi_{F,ST})} - 1\right]^{-1} \quad (7)$$

where $\Phi_{F,OBS}$ represents observed yields. The results in different solvents are shown in Table 1.

In order to determine fluorescence quantum yields of DPB at different temperatures, a characterization of the dependence of the DPB absorption spectrum on temperature is required. In both MCH and toluene, absorption spectra of DPB were measured as a function of temperature (Figure 7). The solution concentrations were selected such that observed absorbances were high enough to minimize effects of experimental uncertainties. The measurements at a high DPB concentration (Figure 7 inset) are to emphasize only the extreme red onset region of the absorption spectrum. Because the temperatures used in the absorption measurements do not match exactly those of the fluorescence measurements, the required optical density values at the temperatures used in the fluorescence measurements were obtained through interpolations.

For DPB in both MCH and toluene, observed fluorescence quantum yields as a function of temperature are shown in Figure 6. If the observed yields of the s-trans conformer are assumed to be excitation wavelength independent, the yields of the s-cis conformer can be calculated from the observed yields and the known temperature dependence of the x_{SC}/x_{ST} ratio (eq 7). Results thus obtained are also shown in Figure 6. The $\Phi_{F,SC}/\Phi_{F,ST}$ ratio is temperature dependent for DPB in both MCH and toluene.

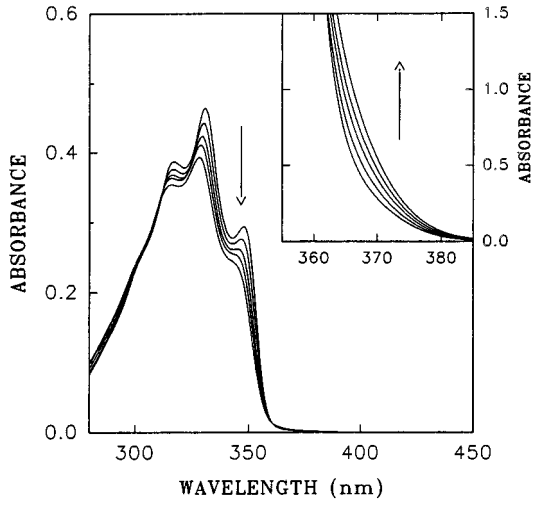

Figure 7. Observed absorption spectra of DPB in MCH at representative temperatures of (in the arrow direction) 20.1, 40.2, 60.3, 80.4, and 100.8 °C. Shown in the inset are observed spectra (red onset only) of a high-concentration DPB solution in MCH at temperatures of (in the arrow direction) 20.0, 40.0, 60.0, 80.1, and 100.1 °C.

Conformational Equilibrium. The quantitative separation of fluorescence spectral mixtures and the determination of fluorescence quantum yields of the two conformers at different temperatures allow an evaluation of the ground state conformational equilibrium. The equilibrium constant *K* (Scheme 1) can be related to fluorescence parameters as follows:

$$K = c_{SC}/c_{ST} = [(x_{SC}/x_{ST})/(\Phi_{F,SC}/\Phi_{F,ST})]/(\epsilon_{SC}/\epsilon_{ST}) \quad (8)$$

where *c* denotes equilibrium concentrations. With an assumption that $\epsilon_{SC}/\epsilon_{ST}$ ratios at the excitation wavelengths in the extreme red onset region of the DPB absorption spectrum are temperature independent, thermodynamic parameters of the DPB ground state s-trans ⇄ s-cis equilibrium can be determined from a plot of $\ln[(x_{SC}/x_{ST})/(\Phi_{F,SC}/\Phi_{F,ST})]$ vs $1/T$.

$$\ln[(x_{SC}/x_{ST})/(\Phi_{F,SC}/\Phi_{F,ST})] = -\Delta H/RT + \Delta S/R + \ln(\epsilon_{SC}/\epsilon_{ST}) \quad (9)$$

where ΔH and ΔS are enthalpy and entropy differences between the two conformers. Plots based on eq 9 for DPB in MCH and toluene are shown in Figure 8. Linear least-squares regressions yield ΔH values of 1.9 ± 0.1 and 2.3 ± 0.3 kcal/mol for DPB in MCH and toluene, respectively.

Calculations. The ground state conformational equilibrium in DPB was also evaluated on the basis of *ab initio* calculations.[30] Computations were performed in the environment of the *Spartan* software package. In the calculations, molecular energy and geometry were first optimized using the AM1 semiempirical method[31] and then further optimized using the *ab initio* method[30] with the STO-3G minimum basis set.

Energy and geometry optimization for DPB s-trans and s-cis conformers was performed without any constraints. The results show that both conformers are planar, with the energy of the s-cis conformer being 2.21 kcal/mol higher than that of the s-trans conformer. The calculated energy difference between the two conformers is in surprisingly good agreement with those from fluorescence results. Other structural parameters from the

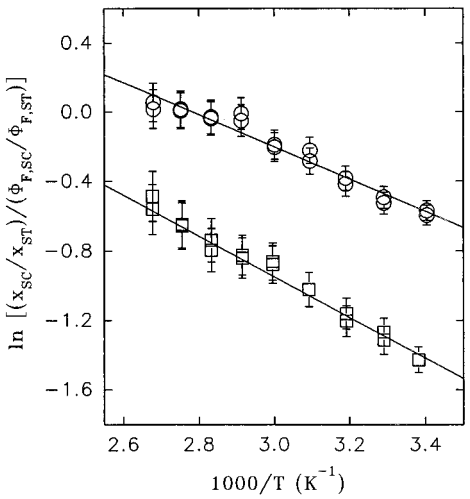

Figure 8. Plots to obtain ground state conformational enthalpy differences for DPB in MCH (○, $i = 2.58$, $s = -927$, and $\gamma = 0.979$) and toluene (□, $i = 2.6$, $s = -1170$, and $\gamma = 0.992$).

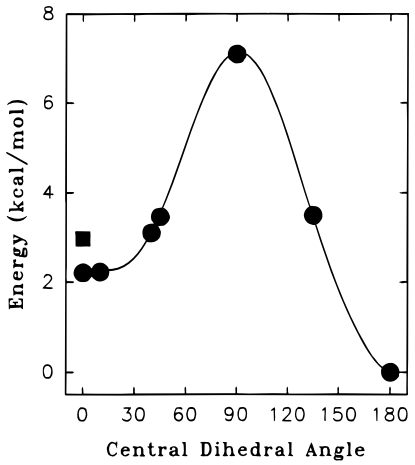

Figure 9. Conformational energies of DPB as a function of dihedral angle $C_1C_4C_3C_2$ (Table 2) from *ab initio* calculations using the STO-3G minimum basis set.

calculations are shown in Table 2. For the parent 1,3-butadiene, it was shown[32] that the optimized dihedral angle $C_1C_4C_3C_2$ is affected by the flexibility of the $C_1C_4C_3$ and $C_4C_3C_2$ angles. The possibility of a similar behavior in DPB was examined by performing an energy and geometry optimization of the s-cis conformer with the angles $C_{15}C_1C_4$, $C_1C_4C_3$, $C_4C_3C_2$, and $C_3C_2C_{16}$ constrained at the same values as those in the optimized geometry of the s-trans conformer (Table 2). It is found that the s-cis conformer is still planar even under such a constraint. However, the calculated energy is higher for the s-cis conformer structure with the angles fixed (Figure 9).

Conformational energies of DPB at different dihedral angles are shown in Figure 9. The results are from calculations in which the dihedral angle $C_1C_4C_3C_2$ is fixed at the specified values. The energy barrier separating the two conformers is 7.1 kcal/mol relative to the s-trans conformer (Figure 9). Calculated structural parameters for DPB at the dihedral angle of 90° are also shown in Table 2.

Discussion

At a constant temperature, a chemometric separation of conformer fluorescence spectral mixtures using spectral data matrices consisting of observed spectra at different excitation wavelengths is subject to no intrinsic limitations. In the absence of experimental noise, observed fluorescence spectra are truly linear combinations of the spectra of individual conformers. However, nonlinear effects due to spectral broadening can be significant when a data matrix is generated by including experimental spectra at different temperatures. Thus, in our data treatments discussed above separations of fluorescence spectral mixtures were carried out at individual temperatures. While it might be argued that the generation of pure conformer spectra

TABLE 2: Structural Description of DPB Conformers from *ab Initio* Calculations

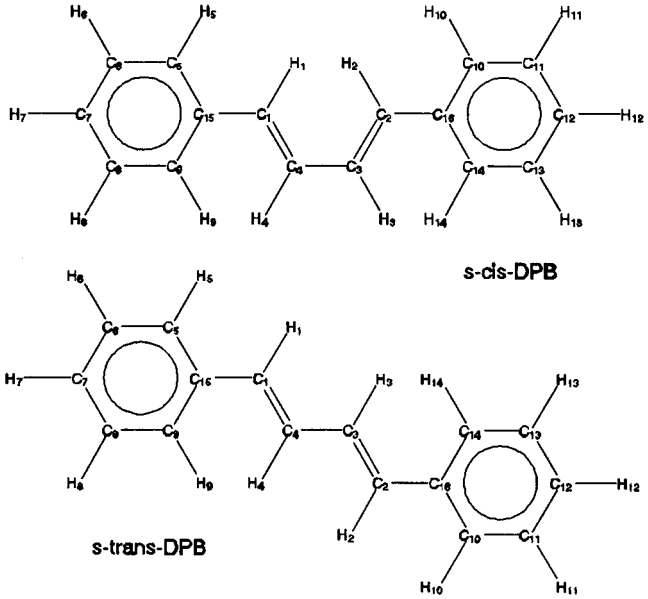

	central dihedral angle			
	0°	0°[a]	90°	180°
Bond Lengths (Å)				
$C_{15}-C_1$	1.4928	1.4929	1.4967	1.4920
$C_1=C_4$	1.3235	1.3239	1.373	1.3235
C_4-C_3	1.4836	1.4943	1.5061	1.4803
$C_3=C_2$	1.3235	1.3239	1.3172	1.3235
C_2-C_{16}	1.4928	1.4929	1.4967	1.4920
H_1C_1	1.0829	1.0810	1.0841	1.0840
H_4C_4	1.0825	1.0821	1.0850	1.0826
H_3C_3	1.0825	1.0820	1.0851	1.0826
H_2C_2	1.0829	1.0810	1.0841	1.0840
Bond Angles (deg)				
$C_9H_{15}C_1$	123.2	122.9	123.0	123.0
$C_5C_{15}C_1$	118.7	119.0	118.8	118.9
$C_{15}C_1C_4$	126.6	(126.9)	126.8	126.9
$C_1C_4C_3$	126.2	(123.4)	123.7	123.4
$C_4C_3C_2$	126.2	(123.4)	123.7	123.4
$C_3C_2C_{16}$	126.6	(126.9)	126.8	126.9
$C_2C_{16}C_{10}$	118.7	119.0	118.8	118.9
$C_2C_{16}C_{14}$	123.2	122.9	123.0	123.0
$H_9C_9C_{15}$	120.1	120.0	120.1	120.0
$H_5C_5C_{15}$	119.2	119.3	119.2	119.2
$C_{15}C_1H_1$	113.9	113.3	114.2	114.4
$H_1C_1C_4$	119.5	119.7	118.9	118.7
$C_1C_4H_4$	119.6	120.9	120.7	121.0
$H_4C_4C_3$	114.2	115.7	115.6	115.7
$C_4C_3H_3$	114.1	115.7	115.6	115.7
$H_3C_3C_2$	119.6	120.9	120.7	121.0
$C_3C_2H_2$	119.5	119.7	118.9	118.7
$H_2C_2C_{16}$	113.9	113.3	114.2	114.4
$H_{10}C_{10}C_{16}$	119.2	119.3	119.3	119.2
$H_{14}C_{14}C_{16}$	120.1	120.0	120.1	120.0
Dihedral Angles (deg)				
$C_9C_{15}C_1C_4$	0.0	0.0	1.9	0.0
$C_5C_{15}C_1C_4$	180.0	180.0	178.1	180.0
$C_{15}C_1C_4C_3$	180.0	180.0	179.2	180.0

[a] Calculated by fixing four angles at values (shown in parentheses) the same as those in the optimized structure of the s-trans conformer.

at different temperatures through interpolations from those spectra obtained at room and high temperatures is less than ideal, potential errors associated with the approach are likely insignificant because the spectra at room and high temperatures are quite similar (Figure 3).

The calculation of fluorescence quantum yields of the s-cis conformer on the basis of eq 7 involves an assumption that the fluorescence yield of the s-trans conformer is excitation wavelength independent. The assumption is somewhat justified by the fact that yields obtained at different excitation wavelengths in the main band of the observed DPB absorption spectrum are essentially the same.

Because of the difference between the two conformers in the temperature dependence of fluorescence quantum yields, the enthalpy difference for the ground state conformational equilibrium cannot be determined accurately by treating the $\Phi_{F,SC}/\Phi_{F,ST}$ ratio as a temperature independent constant.[23] For DPB, neglecting the temperature dependence of the $\Phi_{F,SC}/\Phi_{F,ST}$ ratio will result in an underestimation of the enthalpy difference (1.4 and 1.2 kcal/mol vs the correct values of 1.9 and 2.3 kcal/mol in MCH and toluene, respectively). Similarly, the enthalpy difference could be overestimated in other systems if the temperature dependence of fluorescence quantum yield $\Phi_{F,SC}/\Phi_{F,ST}$ is in the opposite direction.

While the inclusion of the temperature dependence of $\Phi_{F,SC}/\Phi_{F,ST}$ ratios in the plots shown in Figure 8 is necessary, it also increases the error margins. Since $\Phi_{F,SC}$ was calculated from eq 7 and sensitive to uncertainties in $\Phi_{F,OBS}/\Phi_{F,ST}$, the thermodynamic parameters obtained from eq 9 are subject to amplified effects of experimental uncertainties in fluorescence quantum yield measurements. Nevertheless, the ΔH values thus determined are still largely correct because the major contribution in eq 9 is from the temperature dependence of the x_{SC}/x_{ST} term, which is less sensitive to experimental uncertainties.

There are systematic curvatures in the plots shown in Figure 8. The results can be fitted with a second-order function better than the linear eq 9 (correlation coefficients of 0.99 with the second-order function vs 0.97 with the linear equation for results in MCH). The curvatures may be real and may be attributed to different mechanisms such as ΔH or $\epsilon_{SC}/\epsilon_{ST}$ being temperature dependent. However, considering the relatively large error margins in the experimental data and the spectral resolution method, we are not in the position to be more precise in this regard. Treatment based on eq 9 serves as a reasonable approximation for the estimation of the thermodynamic parameters.

It is interesting that the *ab initio* calculations predict a planar ground state geometry for the s-cis conformer. Unlike the parent 1,3-butadiene, where changes in the $C_1C_4C_3$ and $C_4C_3C_2$ angles from the optimized values of the s-trans conformer are required for a planar s-cis geometry,[32] the planarity of *s-cis*-DPB is not affected by fixing the same angles in the calculations. Experimentally, fluorescence spectra of the s-cis conformer are structurally similar to those of the s-trans conformer. The results support the notion that the ground state geometry of the s-cis conformer is similar to that of the planar s-trans conformer.[33]

The enthalpy difference between the two conformers is somewhat solvent dependent. The consistently lower fluorescence contributions from *s-cis*-DPB in toluene compared to those in MCH may be explained by the somewhat larger enthalpy difference in toluene. For DPB in both MCH and toluene, the ΔH values are clearly smaller than the enthalpy difference of $\sim$3 kcal/mol for the conformational equilibrium in the parent 1,3-butadiene. For DPH, a molecule closely related to DPB, ΔH values similar to those in 1,3-butadiene were estimated from fluorescence results.[23] However, the accuracy of the ΔH value for DPH is dependent on the validity of the assumption used in the $\ln(x_{SC}/x_{ST})$ vs $1/T$ plots that the $\Phi_{F,SC}/\Phi_{F,ST}$ ratio is a temperature independent constant, while the DPB ΔH values reported here may be affected by the assumption of $\epsilon_{SC}/\epsilon_{ST}$ being temperature independent.

Acknowledgment. Financial support from the National Science Foundation (CHE-9320558) and the donors of the Petroleum Research Fund, administered by the American Chemical Society, is gratefully acknowledged. Cory A. Lytle is a participant in the Summer Undergraduate Research Program sponsored jointly by the National Science Foundation (CHE-9100387) and by Clemson University.

References and Notes

(1) For a review see: (a) Hudson, B. S.; Kohler, B. E.; Schulten, K. in *Excited States*; Lim, E. C., Ed.; Academic Press: New York, 1982; Vol. 6, p 1. (b) Hudson, B. S.; Kohler, B. E. *Annu. Rev. Phys. Chem.* **1974**, *25*, 437. (c) Kohler, B. E. *Chem. Rev.* **1993**, *93*, 41.

(2) (a) Hudson, B. S.; Kohler, B. E. *Chem. Phys. Lett.* **1972**, *14*, 299. (b) Hudson, B. S.; Kohler, B. E. *J. Chem. Phys.* **1973**, *59*, 4984.

(3) Saltiel, J.; Sun, Y.-P. In *Photochromism, Molecules and Systems*; Dürr, H., Bouas-Laurent, H., Eds.; Elsevier: Amsterdam, 1990; p 64.

(4) Allen, M. T.; Whitten, D. G. *Chem. Rev.* **1989**, *89*, 1691.

(5) (a) Bennett, J. A.; Birge, R. R. *J. Chem. Phys.* **1980**, *73*, 4234. (b) Amirav, A.; Sonnenschein, M.; Jortner, J. *Chem. Phys.* **1986**, *102*, 305. (c) Itoh, T.; Kohler, B. E. *J. Phys. Chem.* **1987**, *91*, 1760. (d) Anderson, R. J. M.; Holtom, G. R.; McClain, W. M. *J. Chem. Phys.* **1979**, *70*, 4310. (e) Swofford, R. L.; McClain, W. M. *J. Chem. Phys.* **1973**, *59*, 5740. (f) Fang, H. L.; Gustafson, T. L.; Swofford, R. L. *J. Chem. Phys.* **1983**, *78*, 1663.

(6) Heimbrook, L. A.; Kohler, B. E.; Spiglanin, T. A. *Proc. Natl. Acad. Sci. U.S.A.* **1983**, *80*, 4580.

(7) Waldeck, D. H. *Chem. Rev.* **1991**, *91*, 415.

(8) Shepanski, J. F.; Keelan, B. W.; Zewail, A. H. *Chem. Phys. Lett.* **1983**, *103*, 9.

(9) Velsko, S. P.; Fleming, G. R. *J. Chem. Phys.* **1982**, *76*, 3553.

(10) Keery, K. M.; Fleming, G. R. *Chem. Phys. Lett.* **1982**, *93*, 322.

(11) (a) Gehrke, Ch.; Mohrschladt, R.; Schroeder, J.; Troe, J.; Vöhringer, P. *Chem. Phys.* **1991**, *152*, 45. (b) Troe, J.; Amirav, A.; Jortner, J. *Chem. Phys. Lett.* **1985**, *115*, 245. (c) Gehrke, Ch.; Schroeder, J.; Schwarzer, D.; Troe, J.; Voss, F. *J. Chem. Phys.* **1990**, *92*, 4805.

(12) Rulliere, C.; Declemy, A.; Kottis, Ph. *Laser Chem.* **1985**, *5*, 185.

(13) Schroeder, J. *Ber. Bunsen-Ges. Phys. Chem.* **1991**, *95*, 233.

(14) Dauben, W. G.; McInnis, E. L.; Michno, D. M. In *Rearrangement in Ground and Excited States*; de Mayo, P., Ed.; Academic Press: New York, 1980; Vol. 3, p 91.

(15) For example: (a) Squillacote, M. E.; Sheridan, R. S.; Chapman, O. L.; Anet, F. A. L. *J. Am. Chem. Soc.* **1979**, *101*, 3657. (b) Mui, P. W.; Grunwald, E. *J. Am. Chem. Soc.* **1982**, *104*, 6562. (c) Sun, Y.-P.; Sears, D. F., Jr.; Saltiel, J. *J. Am. Chem. Soc.* **1988**, *110*, 6277. (d) Arnold, B. R.; Balaji, V.; Michl, J. *J. Am. Chem. Soc.* **1990**, *112*, 1808. (e) Fisher, J. J.; Michl, J. *J. Am. Chem. Soc.* **1987**, *109*, 1056.

(16) Breulet, J.; Lee, T. J.; Schaefer, H. F., III. *J. Am. Chem. Soc.* **1984**, *106*, 6250.

(17) Wiberg, K. B.; Rosenberg, R. E.; Rablen, P. R. *J. Am. Chem. Soc.* **1991**, *113*, 2890, and references cited therein.

(18) Jacobs, H. J. C.; Havinga, E. *Adv. Photochem.* **1979**, *11*, 305.

(19) Mazzucato, U.; Momicchioli, F. *Chem. Rev.* **1991**, *91*, 1679.

(20) Wallace-Williams, S. E.; Moller, S.; Goldbeck, R. A.; Hanson, K. M.; Lewis, J. W.; Yee, W. A.; Kliger, D. S. *J. Phys. Chem.* **1993**, *97*, 9587.

(21) Sun, Y.-P.; Bunker, C. E.; Wickremesinghe, P. L.; Rollins, H.; Lawson, G. E. *J. Phys. Chem.* **1995**, *99*, 3423.

(22) Møller, S.; Yee, W. A.; Goldbeck, R. A.; Wallace-Williams, S. E.; Lewis, J. W.; Kliger, D. S. *Chem. Phys. Lett.* **1995**, *243*, 579.

(23) Saltiel, J.; Sears, D. F., Jr.; Sun, Y.-P.; Choi, J.-O. *J. Am. Chem. Soc.* **1992**, *114*, 3607.

(24) Hirayama, S.; Shobatake, K.; Tabayashi, K. *Chem. Phys. Lett.* **1985**, *121*, 228, and references cited therein.

(25) For reviews, see: (a) Ramos, L. S.; Beebe, K. R.; Carey, W. P.; Sanchez, E. M.; Erickson, B. C.; Wilson, B. E.; Wangen, L. E.; Kowalski, B. R. *Anal. Chem.* **1986**, *58*, 294R. (b) McGown, L. B.; Warner, I. M. *Anal. Chem.* **1990**, *62*, 255R. (c) Brown, S. D.; Blank, T. B.; Sum, S. T.; Weyer, L. G. *Anal. Chem.* **1994**, *66*, 315R.

(26) For typical applications to conformer spectra, see: (a) Saltiel, J.; Eaker, D. W. *J. Am. Chem. Soc.* **1984**, *106*, 7624. (b) Ghiggino, K. P.; Skilton, P. F.; Fischer, E. *J. Am. Chem. Soc.* **1986**, *108*, 1146. (c) Sun, Y.-P.; Sears, D. F., Jr.; Saltiel, J.; Mallory, F. B.; Mallory, C. W.; Buser, C. A. *J. Am. Chem. Soc.* **1988**, *110*, 6974. (d) Spalletti, A.; Bartocci, G.; Masetti, F.; Mazzucato, U.; Cruciani, G. *Chem. Phys.* **1992**, *160*, 131.

(27) For typical other applications: (a) Sylvestre, E. A.; Lawton, W. H.; Maggio, M. S. *Technometrics* **1974**, *16*, 353. (b) Ohta, N. *Anal. Chem.* **1973**, *45*, 553. (c) Osten, D. W.; Kowalski, B. R. *Anal. Chem.* **1984**, *56*, 991. (d) Aartsma, T. J.; Gouterman, M.; Jochum, C.; Kwiram, A. L.; Pepich, B. V.; Williams, L. D. *J. Am. Chem. Soc.* **1982**, *104*, 6281. (e) Sun, Y.-P.; Sears, D. F., Jr.; Saltiel, J. *J. Am. Chem. Soc.* **1989**, *111*, 706. (f) Vandeginste, B.; Essers, R.; Bosman, T.; Reijnen, J.; Kateman, G. *Anal. Chem.* **1985**, *57*, 971. (g) Tauler, R.; Kowalski, B.; Fleming, S. *Anal. Chem.* **1993**, *65*, 2040. (h) Bunker, C. E.; Hamilton, N. B.; Sun, Y.-P. *Anal. Chem.* **1993**, *65*, 3460.

(28) Malinowski, E. R. *Factor Analysis in Chemistry*, 2nd ed.; Wiley: New York, 1991.

(29) Lawton, W. H.; Sylvestre, E. A. *Technometrics* **1971**, *13*, 617.

(30) Hehre, W. J.; Radom, L.; Schleyer, P. V. R.; Pople, J. A. *Ab Initio Molecular Orbital Theory*; Wiley: New York, 1985.

(31) Dewar, M. J. S.; Zoebisch, E. G.; Healy, E. F.; Stewart, J. J. P. *J. Am. Chem. Soc.* **1985**, *107*, 3902.

(32) Radom, L.; Pople, J. A. *J. Am. Chem. Soc.* **1970**, *92*, 4786.

(33) Yee, W. A.; Horwitz, J. S.; Goldbeck, R. A.; Einterz, C. M.; Kliger, D. S. *J. Phys. Chem.* **1983**, *87*, 380.